# Superconductivity and magnetism of a body-centered tetragonal $ErRh_4B_4$ single crystal. II. Large anisotropy of $H_{c2}$

H. Iwasaki and Y. Muto
*The Research Institute for Iron, Steel and Other Metals, Tohoku University, Sendai 980, Japan*
(Received 14 August 1985)

Upper critical field $H_{c2}$ and magnetization are measured on a single crystal of body-centered tetragonal (bct) $ErRh_4B_4$ which is an antiferromagnetic superconductor and behaves metamagnetically in the $c$ plane under a magnetic field below $T_N$. The temperature dependences of $H_{c2}$ along the [001] and [100] axes are roughly similar to each other in that both $H_{c2}(T)$ take maxima with decreasing temperature but the magnitude of $H_{c2}$ along the [001] axis is quite large compared to that along the [100] axis. Furthermore, the angular dependence of $H_{c2}$ in the $c$ plane shows the fourfold anisotropy above $T_N$ and the complex twofold anisotropy below $T_N$. The anisotropy of $H_{c2}$ is closely related with that of the magnetization. From the analysis in which the spin polarization due to the $s$-$f$ exchange interaction and the electromagnetic interaction are taken into account it is made clear that the spin polarization plays a very important role in determining $H_{c2}$. The $s$-$f$ exchange constant and the spin-orbit scattering parameter are also determined. It is indicated that the $s$-$f$ exchange interaction is ferromagnetic and the spin-orbit scattering is very strong in the bct $ErRh_4B_4$ crystal. Finally temperature dependence of $H_{c2}$ in the $c$ plane below $T_N$ is qualitatively discussed, being connected with metamagnetism.

## I. INTRODUCTION

Magnetic superconductor $\mathscr{R}Rh_4B_4$ ($\mathscr{R}$ is a rare-earth metal) compounds have been intensively studied in order to understand the interplay between superconductivity and magnetism.[1] So far, three kinds of $\mathscr{R}Rh_4B_4$ compounds have been discovered: (i) The $CeCo_4B_4$ type with primitive tetragonal (pt) structure.[2] The pt $\mathscr{R}Rh_4B_4$ compounds are the most familiar magnetic superconductors and there are many studies on these compounds. $ErRh_4B_4$ with this structure is a typical ferromagnetic superconductor and shows a reentrant behavior.[3] (ii) The $LuRu_4B_4$ type with body-centered tetragonal (bct) structure.[4] Although the bct phase has been stabilized only in the pseudoternary $\mathscr{R}(Ru_{1-x}Rh_x)_4B_4$ system,[4] we succeed in obtaining $ErRh_4B_4$ with this structure which is an antiferromagnetic superconductor.[5] (iii) The $LuRh_4B_4$ type with orthorhombic structure.[6] The superconducting transition temperatures of several compounds have been reported.[7]

It is expected that in the magnetic superconductor the magnetic anisotropy influences superconducting properties such as the upper critical field $H_{c2}$ because exchange interaction exists between the superconducting electrons and the magnetic ions. It has been highly desirable to make a study of a single crystal of the magnetic superconductor in order to obtain precise information on the interplay between superconductivity and magnetism.

Recently, we succeeded in preparing a bct $ErRh_4B_4$ single crystal[8,9] and found for the first time the anisotropy of $H_{c2}$ among a number of antiferromagnetic superconductors. In this paper we discuss the relationship between the anisotropy of $H_{c2}$ and magnetization. The experimental procedure is briefly described in Sec. II; the experimental results are presented in Sec. III and discussions are given in Sec. IV. A brief report of the $H_{c2}$ anisotropy was reported elsewhere.[9] Experimental results on magnetization and a detailed analysis are described in the preceding paper[10] referred to as paper I.

## II. EXPERIMENTAL

$H_{c2}$ was measured by an ac resistive method, sweeping the magnetic field at a constant temperature. $H_{c2}$ was defined by the linearly extrapolated field of the transition curve to zero resistance. A $^3$He-$^4$He dilution refrigerator was used in the measurements below 1 K. The bct $ErRh_4B_4$ single crystal which was synthesized by induction heating is the same as that in the preceding paper I. $LuRh_4B_4$, with the body-centered tetragonal structure, was also synthesized by induction heating, as a reference sample. The bct $LuRh_4B_4$ sample is polycrystalline and was annealed for two weeks at 1050 °C, being covered with a Ta foil and sealed into a quartz tube under Ar atmosphere. This sample contains a small quantity of RhB as an impurity phase.

## III. RESULTS

The residual resistivity just above $T_c$ and the residual resistance ratio (RRR) of the bct $ErRh_4B_4$ sample are $\rho_0 \simeq 65\ \mu\Omega$ cm and a RRR of 1.70, respectively. Those of the bct $LuRh_4B_4$ sample are $\rho_0 \simeq 60\ \mu\Omega$ cm and a RRR of 1.65. These values are roughly common throughout the bct $\mathscr{R}Rh_4B_4$ compounds, and $\rho_0$ is large by a figure compared with those in the pt $\mathscr{R}Rh_4B_4$ compounds. The large residual resistivity suggests that the bct $\mathscr{R}Rh_4B_4$ compounds are dirty superconductors. The superconducting transition temperature $T_c$ and the Néel temperature $T_N$ of the bct $ErRh_4B_4$ sample are 7.80 and 0.65 K, respectively.

The magnetization process of bct $ErRh_4B_4$ has been

 

described in paper I. The results of the magnetization measurements in the superconducting paramagnetic state are summarized as follows. The [001] axis is the hard-magnetization direction. Large fourfold magnetic anisotropy exists in the $c$ plane. The [100] axis is the easy-magnetization direction and the [110] axis is the hard-magnetization direction in the $c$ plane. In the field range in which the sample shows the transition from the superconducting state to the normal one, the magnetization shows anisotropy due to the fourfold magnetic anisotropy. The magnetization values $M(H_{c2})$ at $H_{c2}$ for $\mathbf{H}\|[100]$ and $\mathbf{H}\|[110]$ are nearly equal to each other in spite of the fact that $H_{c2}$ takes different values for both directions.

Below $T_N$ the magnetization curves for $\mathbf{H}\|[100]$ show two-step jumps exhibiting hysteresis for increasing and decreasing fields. Similar magnetization curves with the two-step jumps are also observed for $\mathbf{H}\|[010]$. On the other hand, the magnetization for $\mathbf{H}\|[110]$ shows a one-step jump. The magnetization process observed below $T_N$ is understood as metamagnetism under the fourfold magnetic anisotropy.

Figure 1 shows the temperature dependence of $H_{c2}$ in the [001], [100], and [110] directions. $H_{c2}$ along the [001] direction which is the axis of hard magnetization is very large compared with those in the $c$ plane. It increases monotonically down to 1.5 K, decreases a little at lower temperatures, and is almost constant below $T_N$. The $H_{c2}(T)$ curve in the [100] direction takes a maximum at about 4.5 K and gradually decreases at lower temperatures. The inset in Fig. 1 shows $H_{c2}(T)$ along the [100] and [110] directions around $T_N$ in the enlarged $H_{c2}$ scale. $H_{c2}$ along the [100] direction takes a dip at 0.6 K, which is nearly equal to $T_N$. The anisotropy of $H_{c2}$ is also observed in the $c$ plane. $H_{c2}$ along the [110] direction is always higher than that along the [100] direction above $T_N$. However, $H_{c2}$ along both the [100] and [110] directions coincides at 0.3 K and $H_{c2}$ along the [100] direction is higher than that along the [110] direction below 0.3 K.

The angular dependences of the upper critical field $H_{c2}(\theta)$ in the $c$ plane at 7.0, 4.3, and 0.5 K are shown in Figs. 2(a), 2(b) and 2(c), respectively. $H_{c2}(\theta)$ at 7.0 K just

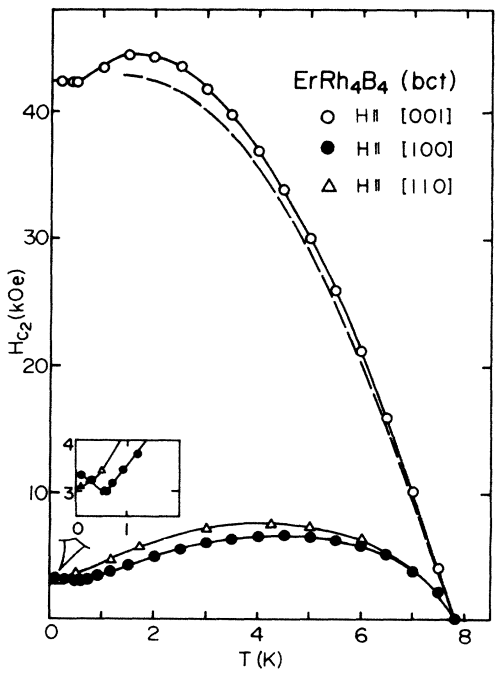


FIG. 1. Temperature dependence of $H_{c2}$ of bct $ErRh_4B_4$ (a) for $\mathbf{H}\|[001]$, $\mathbf{H}\|[100]$, and $\mathbf{H}\|[110]$. The dashed curve in (a) shows $H_{c2}$ after the demagnetization correction. In the inset $H_{c2}$ in the $c$ plane around $T_N$ is shown in the enlarged scale.

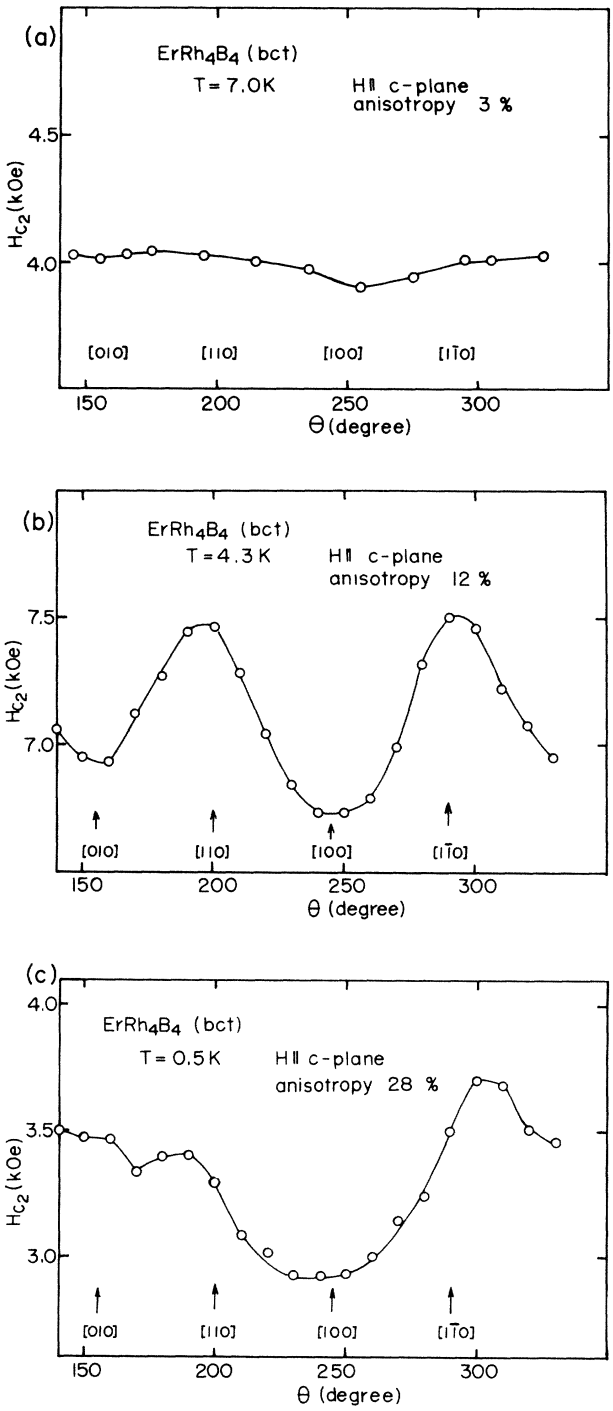


FIG. 2. Angular dependence of $H_{c2}$ of bct $ErRh_4B_4$ (a) at 7.0 K just below $T_c$, (b) at 4.3 K, and (c) at 0.5 K, below $T_N$.

below $T_c$ shows nearly no anisotropy. $H_{c2}(\theta)$ at 4.3 K almost shows the fourfold anisotropy with the magnitude of 12%, where the anisotropy is defined by

$$\frac{H_{c2_{\max}}-H_{c2_{\min}}}{H_{c2_{\min}}} . \quad (1)$$

The minima of $H_{c2}$ appear in the [100] and [010] directions which are the axes of easy magnetization, and the maxima of $H_{c2}$ are in the [110] and [1$\bar{1}$0] directions which are the axes of hard magnetization in the $c$ plane. It should be noted that $H_{c2}$ values are clearly different between the crystallographically equivalent [100] and [010] directions, though both take minima. The discrepancy is beyond the limit of demagnetization correction. This is also observed in the magnetization measurements (see paper I), where the small magnetic anisotropy between the [100] and [010] axes exists in this sample. This is also apparent in the angular dependence of $H_{c2}$ at 0.5 K just below $T_N$. However, Fig. 2(c) shows that $H_{c2}(\theta)$ does not show the fourfold anisotropy, but the complex twofold anisotropy. Only $H_{c2}$ along the [100] direction takes a minimum. The magnitude of anisotropy amounts to 28%.

Figures 3(a) and 3(b) show the temperature dependence of the anisotropy of $H_{c2}$ between principal axes in the $c$ plane and the $a$ plane, respectively. The definition of anisotropy is given in Figs. 3(a) and 3(b). The anisotropy of $H_{c2}$ between the [100] and [110] directions shows significant temperature dependence. This anisotropy is very small at temperatures just below $T_c$, and increases gradually with decreasing temperature. After taking a maximum at 1.5 K, it becomes small again at 0.5 K, because $H_{c2}$ along the [110] direction does not take a maximum, as shown in Fig. 2(c). The anisotropy of $H_{c2}$ between the [100] and [001] directions has strong temperature dependence, as shown in Fig. 3(b). It is extremely large, exceeding 800% at 1.7 K.

In Fig. 4 the magnetization values at $H_{c2}$,$M(H_{c2})$ are plotted as a function of the temperature for $\mathbf{H}\|[100]$, $\mathbf{H}\|[110]$, and $\mathbf{H}\|[001]$. $M(H_{c2})$ was defined by using the magnetization measurements in paper I. As mentioned before, $M(H_{c2})$ almost coincides between the [100] and [110] directions. This indicates that in the $c$ plane superconductivity begins to be destroyed by the generation of a certain magnitude of the magnetization at every temperature. It should be noted that, exactly speaking, $M(H_{c2})$ for $\mathbf{H}\|[110]$ is a little smaller than that for $\mathbf{H}\|[100]$. $M(H_{c2})$ is very small for $\mathbf{H}\|[001]$, whereas $H_{c2}$ is extremely high compared with that in the $c$ plane.

Finally, the experimental results of the bct $LuRh_4B_4$ sample are described. $\rho_0$ and the RRR are almost the same as that of the bct $ErRh_4B_4$ single crystal, as described before. Figure 5 shows the temperature dependence of $H_{c2}$. The gradient of $H_{c2}$ is $(-dH_{c2}/dT)_{T_c}=20.8$ kOe/K, where $T_c$ is 8.61 K. The gradient of $H_{c2}$ is much larger than that of $LuRh_4B_4$ with primitive tetragonal structure[11] and may come from the dirtiness of the sample as indicated by the high resistivity of this sample. The dashed-dotted curve shows $H_{c2}$ in the dirty limit by the Werthamer, Helfand, and Hohenberg

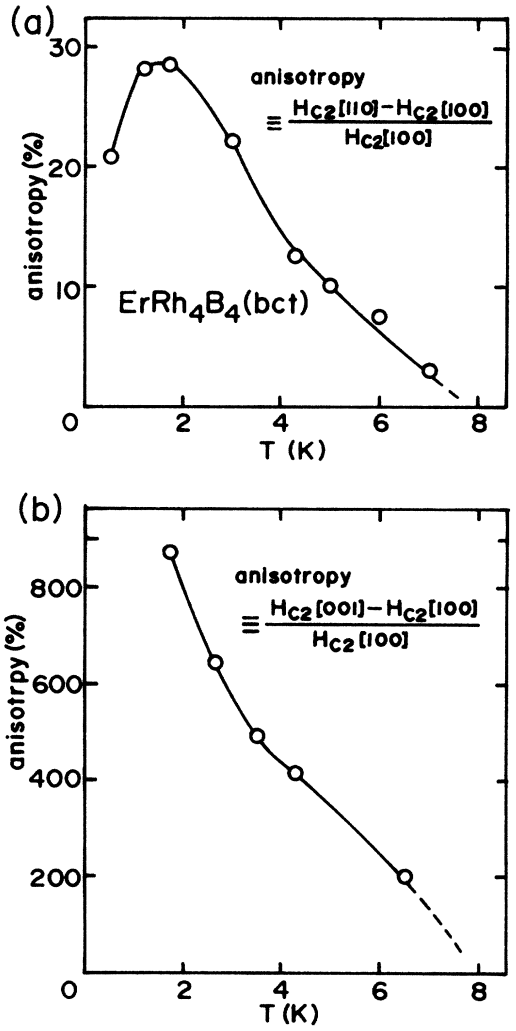


FIG. 3. Temperature dependence of the anisotropy of $H_{c2}$ (a) in the $c$ plane and (b) in the $a$ plane.

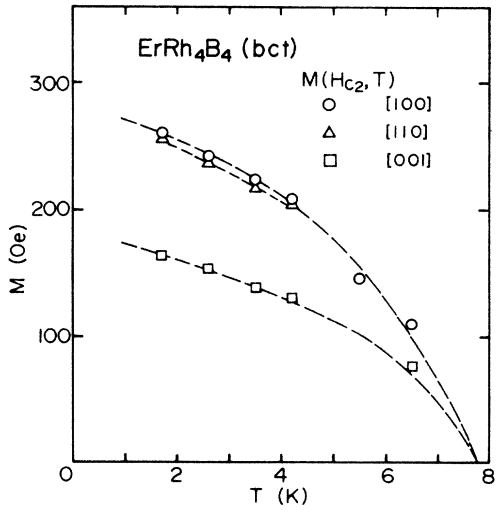


FIG. 4. Temperature dependence of the magnetization at $H_{c2}$ for $\mathbf{H}\|[100]$, $\mathbf{H}\|[110]$, and $\mathbf{H}\|[001]$.

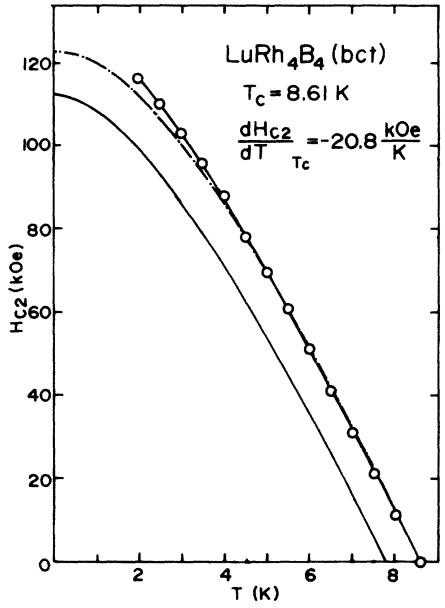


FIG. 5. Temperature dependence of $H_{c2}$ of bct $LuRh_4B_4$. The dashed-dotted curve shows $H_{c2}$ in the dirty limit by WHH theory. The solid curve shows orbital critical field $H_{c2}^*$ of the hypothetical nonmagnetic bct $ErRh_4B_4$ with $T_c=7.80$ K and $-(dH_{c2}/dT)_{T_c}=20.8$ kOe/K.

(WHH) theory.[12] This curve corresponds to the orbital upper critical field. Though $H_{c2}(0)$, estimated from the theoretical curve, is 123 kOe, the experimental data are slightly higher than the theoretical curve.

## IV. DISCUSSION

### A. Anisotropy of $H_{c2}$ of bct $ErRh_4B_4$ above $T_N$

The large anisotropy of $H_{c2}$ between the [100] and [001] directions and the fourfold anisotropy of $H_{c2}$ in the $c$ plane can never be explained as long as the effect of the anisotropic magnetization is not considered, because the crystal structure of the bct $\mathscr{R}Rh_4B_4$ compounds has nearly cubic symmetry as a whole.

In order to explain the large anisotropy of $H_{c2}$ observed in bct $ErRh_4B_4$, we need to take account of both effects of the electromagnetic interaction[13] and the spin polarization due to the $s$-$f$ exchange interaction.[14,15] The bct $\mathscr{R}Rh_4B_4$ compounds are a dirty superconductor, as described in Sec. III. Therefore, in the analysis we use the following expression which holds for the dirty limit[16]:

$$H_{c2}(T)=H_{c2}^*(T)-4\pi M(H_{c2},T) -A[H_{c2}(T)-I'M(H_{c2},T)]^2 , \quad (2)$$

where

$$A=0.022\alpha/\lambda_{s.o.}T_{c0} \quad (3)$$

and

$$I'=4\pi+I , \quad I=(g_J-1)I_0/2Ng_J\mu_B^2 , \quad (4)$$

where $\alpha$ and $\lambda_{s.o.}$ are the Maki parameter and the spin-orbit scattering parameter, respectively, $T_{c0}$ is the superconducting transition temperature of nonmagnetic bct $\mathscr{R}Rh_4B_4$, $N$ is the number of Er spins per unit volume, and $g_J$ is the Landé $g$-factor. The term $4\pi M$ represents the effect of the electromagnetic interaction and the term $IM$, the effect of the spin polarization due to the $s$-$f$ exchange interaction, where $I$ is proportional to the $s$-$f$ exchange constant $I_0$. It should be noted that the electromagnetic interaction behaves not only as an orbital pair-breaking mechanism shown by the second term of Eq. (2) but also as the spin paramagnetic one containing the third term of Eq. (2). On the other hand, the $s$-$f$ exchange interaction which is contained in the third term of Eq. (2) behaves as a spin paramagnetic pair-breaking mechanism. $H_{c2}^*$ is the upper critical field limited by orbital effect only.

$H_{c2}(T)$ of bct $LuRh_4B_4$ which is shown in Fig. 5 is utilized for $H_{c2}^*(T)$ because both its resistivity and its residual resistance ratio are almost the same between the bct $ErRh_4B_4$ and the bct $LuRh_4B_4$ samples, as mentioned in Sec. III. Though $H_{c2}$ of bct $LuRh_4B_4$ in the experiments is slightly higher than the orbital upper critical field $H_{c2}^*$ by the WHH theory, the following analysis is performed on the basis of the theoretical $H_{c2}^*$. It is necessary to correct the discrepancy of the superconducting transition temperature between bct $ErRh_4B_4$ ($T_c=7.80$ K) and bct $LuRh_4B_4$ ($T_{c0}=8.61$ K). Since $(-dH_{c2}/dT)_{T_c}$ does not explicitly depend on $T_c$ in the dirty limit according to the Bardeen-Cooper-Schrieffer – Ginzburg-Landau-Abrikosov-Gor'kov (BCS-GLAG) theory, $(-dH_{c2}/dT)_{T_c}$ is assumed to be almost constant even if $T_c$ changes a little. Therefore, $H_{c2}^*(T)$ is the orbital upper critical field of the hypothetical nonmagnetic superconductor bct $ErRh_4B_4$ with $T_c=7.80$ K and $(-dH_{c2}/dT)_{T_c}=20.8$ kOe/K, which is shown by the solid curve in Fig. 5. Furthermore, it is also implicitly assumed that $H_{c2}^*$ has no anisotropy because the crystal structure of the bct compounds has nearly cubic symmetry as a whole.

The experimental results of $H_{c2}$ shown in Fig. 1 are analyzed on the basis of Eq. (2) by use of $M(H_{c2})$ shown in Fig. 4. In order to explain the anisotropy of $H_{c2}$ observed between the [100] and [001] axes, the values of the parameters $I'$ and $A$ are determined under the conditions $H_{c2}^*=H_{c2}^*[100]=H_{c2}^*[001]$ at every temperature. The two solutions with positive and negative signs are obtained on $I'$. The mean values of the parameters obtained at several temperatures are $I'=1112$, $A=1.1\times10^{-6}$ and $I'=-140$, $A=1.05\times10^{-4}$. In order to determine the solution having the physical meaning, the temperature dependence of $H_{c2}$ along the [110] direction and the angular dependence of $H_{c2}$ in the $c$ plane are calculated by Eq. (2), using each set of parameters $[I',A]$. The calculated results, together with the experimental results, are shown in Figs. 6 ($H_{c2}(T)$ along the [110] direction) and 7 [$H_{c2}(\theta)$ in the $c$ plane]. It is clear that, while $I'$ with negative sign cannot explain the experimental results, $I'$ with positive sign does. Because the value of $I'$ is much larger than $4\pi$, $I'$ in Eq. (4) can be regarded as $I$. The $s$-$f$ exchange constant $I_0$ and the parameter $\lambda_{s.o.}$ are estimated

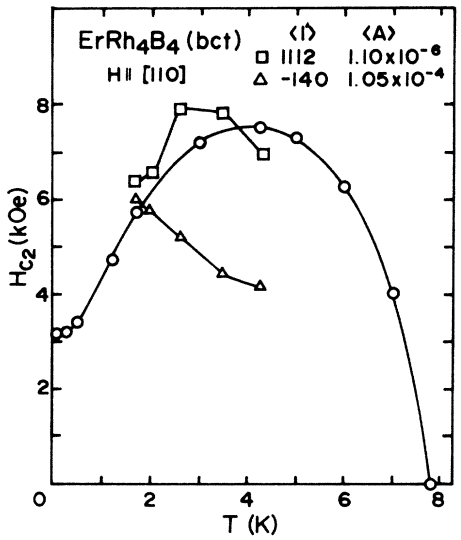


FIG. 6. Comparison of the experimental $H_{c2}$ with the calculated one for $\mathbf{H}\|[110]$. Only the solution with a positive $I'$ value can explain the experimental results.

to be 74 K and $\lambda_{s.o.}=2.81$ by use of Eqs. (3) and (4). The positive sign of $I'$ indicates that the exchange interaction between the conduction electrons and the magnetic spins is ferromagnetic. The large $\lambda_{s.o.}$ value also indicates that the spin-orbit scattering is very strong in this crystal.

Figure 8 shows the contributions of both the electromagnetic interaction and the spin polarization due to the $s$-$f$ exchange interaction to $H_{c2}$ along the [001] and the [100] axes. It is important that $H_{c2}^{*}$ of hypothetical nonmagnetic bct $ErRh_4B_4$ (dashed curve) is greatly reduced by the effect of the spin polarization due to the $s$-$f$ exchange interaction. The arrows show the contribution of the spin polarization to $H_{c2}$ along the [001] and [100] axes. The contribution of the electromagnetic interaction represented by $4\pi M$ is much smaller compared to that of the spin polarization due to the $s$-$f$ exchange interaction. It should be pointed out that the experimental value along

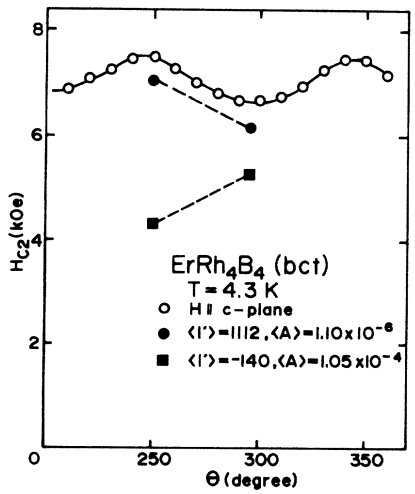


FIG. 7. Comparison of the experimental result of $H_{c2}(\theta)$ with the calculated one. From this result and Fig. 6 the solution with a negative $I'$ value is discarded.

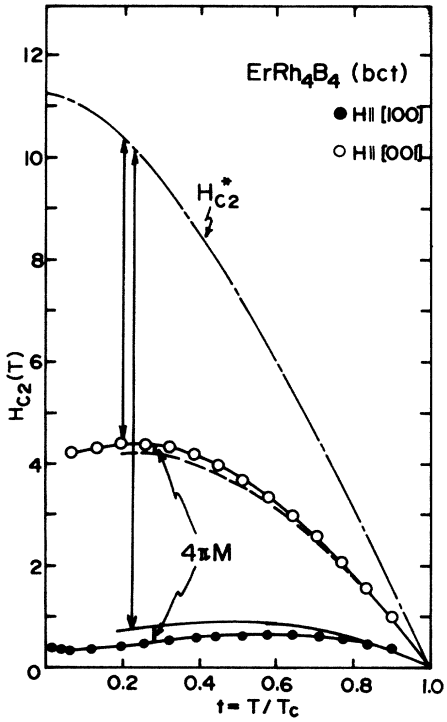


FIG. 8. Contribution of the spin polarization due to the $s$-$f$ exchange interaction and the electromagnetic interaction to $H_{c2}$. The arrows show effects of the spin polarization. The contribution of the electromagnetic interaction is represented by $4\pi M$.

the [001] direction corresponds to $B_{c2}(T)$ because of the demagnetization and that the dashed curve represents the real $H_{c2}(T)$. It should be also noted that the experimental $H_{c2}(T)$ along the [100] direction is real $H_{c2}(T)$ and the solid curve represents $B_{c2}(T)$. It is concluded that $H_{c2}$ along the [100] axis is almost decisively determined by the spin polarization effect and this effect also plays an important role in $H_{c2}$ in the [001] axis. The analysis of $H_{c2}$ is given for the temperature above $T_N$. However, those pair-breaking mechanisms will work for temperature below $T_N$.

### B. Temperature dependence of $H_{c2}$ of bct $ErRh_4B_4$ below $T_N$

As shown in Fig. 1, $H_{c2}$ along the [100] direction increases and $H_{c2}$ along the [110] direction decreases slightly with decreasing temperature below $T_N$. $H_{c2}$ along the [110] direction becomes lower than that along the [100] direction below 0.3 K. These results are qualitatively understood as follows.

As described in the paper I, the magnetization process below $T_N$ is understood as metamagnetism. Superconductivity coexists with the intermediate ferrimagnetic state with the magnetization of $M_0/2$ and is quenched by the occurrence of the induced ferromagnetic order for $\mathbf{H}\|[100]$. The field $H_3$ at which the magnetization shows the second jump becomes slightly higher with decreasing temperature (see Fig. 6 in paper I). Therefore, it is understood that $H_{c2}$ for $\mathbf{H}\|[100]$ increases with decreasing temperature below $T_N$. On the other hand, the magneti-

zation shows a one-step jump for H||[110] and superconductivity coexists with the canted ferromagnetic order with the magnetization of $M_0/\sqrt{2}$. The transition width at $H_2$ becomes narrow when the temperature decreases, and the magnetization around the transition increases abruptly at lower temperature. The magnetization after the jump at 0.1 K is larger than that at 0.5 K. Therefore, $H_{c2}$ for H||[110] decreases with decreasing temperature. It is concluded that $H_{c2}$ in the $c$ plane is mainly determined by the effect of the magnetization through the spin polarization both above and below $T_N$.

$H_{c2}$ along the [001] direction decreases just above $T_N$ and is nearly constant below $T_N$, as shown in Fig. 1. It seems that this behavior of $H_{c2}$ is explained neither by the spin polarization effect due to the $s$-$f$ exchange interaction nor by the electromagnetic interaction. As the magnetizations are strongly suppressed for H||[001], and $M(H_{c2})$ is very small compared with that in the $c$ plane (Fig. 4), it is considered that both effects of the electromagnetic interaction and the spin polarization due to the $s$-$f$ exchange interaction are small compared with the case of H||[100] or H||[110]. Therefore, the other pair-breaking mechanisms such as a spin-fluctuation effect, due to the interaction between the magnetic spins, should be considered. It is not certain what kind of mechanism dominates the behavior so that $H_{c2}$ decreases just above $T_N$ with decreasing temperature and is nearly constant below $T_N$, because $M(H_{c2})$ for H||[001] in the temperature range around $T_N$ has not been measured.

## V. CONCLUSION

We have found the large anisotropy of $H_{c2}$ on the bct $ErRh_4B_4$ single crystal, an antiferromagnetic superconductor. $H_{c2}$ along the [001] direction is extremely large compared with that in the $c$ plane and $H_{c2}$ in the $c$ plane has fourfold anisotropy above $T_N$. In order to explain the anisotropy of $H_{c2}$, the electromagnetic interaction and the spin polarization due to the $s$-$f$ exchange interaction are taken into account in the analysis of $H_{c2}$. It becomes clear that the spin polarization is very important in bct $ErRh_4B_4$. The anisotropies of $H_{c2}$, not only between the [001] axis and the [100] axis but also in the $c$ plane, are explained by this analysis. Furthermore, the $s$-$f$ exchange constant $I_0$ and the spin-orbit scattering parameter $\lambda_{so}$ are determined independently. It is confirmed that the exchange interaction between the conduction electrons and the magnetic spins is ferromagnetic and spin-orbit scattering is very strong in bct $ErRh_4B_4$. Furthermore, the temperature dependence of $H_{c2}$ in the $c$ plane below $T_N$ is discussed in connection with metamagnetism.

## ACKNOWLEDGMENTS

We would like to thank Dr. M. Ikebe and Professor M. Tachiki for valuable discussions. This research was supported by a Grant-in-Aid for Special Project Research on *New Superconducting Materials* from the Ministry of Education, Science and Culture, Japan.

[1]For a review, see M. B. Maple, H. C. Hamaker, and L. D. Woolf, in *Superconductivity in Ternary Compounds II*, Vol. 34 of *Topics in Current Physics*, edited by M. B. Maple and O. Fischer (Springer, Berlin, 1982), p. 99.

[2]J. M. Vandenberg and B. T. Matthias, Proc. Natl. Acad. Sci. USA **74**, 1336 (1977).

[3]W. A. Fertig, D. C. Johnston, L. E. DeLong, R. W. McCallum, M. B. Maple, and B. T. Matthias, Phys. Rev. Lett. **38**, 987 (1977).

[4]D. C. Johnston, Solid State Commun. **24**, 699 (1977).

[5]H. Iwasaki, M. Isino, K. Tsunokuni, and Y. Muto, J. Magn. Magn. Mater. **32**, 521 (1983).

[6]K. Yvon and D. C. Johnston, Acta. Crystallogr. B **38**, 247 (1982).

[7]D. C. Johnston and H. B. Mackay, Bull. Am. Phys. Soc. **24**, 390 (1979).

[8]H. Iwasaki, M. Ikebe, and Y. Muto, in *Proceedings of the International Conference LT17 (1984)* edited by U. Eckern, A. Schmid, W. Weber, and H. Hühl (North-Holland, Amsterdam, 1984), p. 87.

[9]H. Iwasaki, M. Ikebe, and Y. Muto, in *Proceedings of the International Conference LT17 (1984)* edited by U. Eckern, A. Schmid, W. Weber, and H. Hühl (North-Holland, Amsterdam, 1984), p. 89.

[10]H. Iwasaki, M. Ikebe, and Y. Muto, preceding paper, Phys. Rev. B **33**, 4669 (1986).

[11]H. R. Ott, A. M. Campbell, H. Rudigier, H. C. Hamaker, and M. B. Maple, Physica **108B**, 751 (1981).

[12]N. R. Werthamer, E. Helfand, and D. C. Hohenberg, Phys. Rev. **147**, 295 (1966).

[13]O. Sakai, M. Tachiki, T. Koyama, H. Matsumoto, and H. Umezawa, Phys. Rev. B **24**, 3830 (1981).

[14]G. Zwicknagl and P. Fulde, Z. Phys. **43**, 23 (1981).

[15]K. Machida, J. Low Temp. Phys. **37**, 583 (1979).

[16]Ø. Fischer, M. Ishikawa, M. Pelizzone, and A. Treyvaud, J. Phys. (Paris) Colloq. **40**, C5-89 (1979).